Quantum Interference of Virtual and Real Amplitudes in a Semiconductor Exciton System

Y. H. Ahn, S. B. Choe, J. C. Woo, and D. S. Kim*
School of Physics, Seoul National University, Seoul 151-742, Korea

S. T. Cundiff and J. M. Shacklette
JILA, University of Colorado and National Institute of Standard and Technology, Boulder, Colorado 80309-0440

Y. S. Lim
Department of Applied Physics, KonKuk University, Chungju, Chungbuk 380-701, Korea
(Received 7 March 2002; published 18 November 2002)

By two-color pulse shaping, we simultaneously create virtual and real amplitudes for excitons in GaAs quantum wells, and monitor population and amplitude by pump-probe and four-wave mixing spectroscopies. Excited-state probability amplitude can be induced by the off-resonant, virtual excitations as well as by the resonant, real excitations. Population modulation in time-domain results from the interference between the virtual and real amplitudes, and the modulation depth reveals the relative contributions of these two amplitudes. The fact that virtual and real amplitudes have a phase difference of 90° is demonstrated directly in time-domain.

DOI: 10.1103/PhysRevLett.89.237403 PACS numbers: 78.67.De, 39.30.+w, 42.50.Md, 71.35.Cc

Even under far off-resonance illumination of a two level system, significant excited-state probability amplitude exists as long as the perturbing field is present. The fact that the virtual amplitude survives, as a function of detuning, long after the absorption becomes practically zero can be understood by the following well-known formula for the steady-state excited-state probability amplitude $c(t)$ [1]:

$$c(t) \propto \frac{E_0 e^{-i\omega t}}{\omega_0 - \omega - i\gamma}. \quad (1)$$

Here, a continuous wave at a frequency ω illuminates a two level system with a resonance frequency ω_0 and a damping constant γ, and the rotating wave approximation is used. Note that at far off-resonance, the polarization is inversely proportional to detuning, whereas the absorption is inversely proportional to the square of the detuning.

Equation (1) contains a fundamental distinction between the far off-resonant virtual and resonant real amplitudes. At resonance [$\omega = \omega_0$ in Eq. (1)], the probability amplitude is always 90° out of phase with the incident wave, thanks to the "imaginary" nature of damping. At large detuning ($|\omega - \omega_0| \gg \gamma$), however, it is either in phase or 180° out of phase. As a result, virtual and real amplitudes are always 90° out of phase from each other for large detuning. Although this is easily observed at radio frequencies in magnetic resonance experiments, to the best of our knowledge, this fundamental distinction has never been directly demonstrated in the time domain for an optical resonance. Understanding the phase relationship between exciting pulses and the resulting probability amplitude is crucial for coherent control experiments [2–6]. Optical nutation experiments show a detuning dependence [7–9], but are not sensitive to the phase shift. The instantaneous phase dynamics of the nonlinear emission have been demonstrated for the exciton in quantum well (QW) systems for the resonant and partially nonresonant excitations [10]. Recently a chirped pulse was used to observe coherent transients in a two level, atomic system [11].

Semiconductor excitonic systems have long been an ideal playground for the theoretical and experimental studies of virtual excitations [12–22]. The large oscillator strength of semiconductors makes it possible to easily perform nonlinear spectroscopies that probe the population and polarizations of the system. In certain cases, semiconductor excitonic systems behave similarly to a two level system, whereas many-body interaction plays essential roles in other instances [23,24].

In this Letter, we use a two-color picosecond pump pulse, with one frequency (ω_1) much below the exciton resonance and the other at the resonance (ω_0) of the heavy-hole (HH) exciton of a GaAs multiple quantum well sample. In this configuration, virtual and real amplitudes can be simultaneously excited [Fig. 1(a)] and their relative strengths can be changed in controllable and systematical ways. Pump-probe (PP) and four-wave mixing (FWM) are performed, changing the detuning and relative strengths of the real and the virtual frequency components. A pronounced beating, whose period exactly follows the inverse detuning and whose depth is determined by the relative strengths of the frequency components, is observed. There exists a 90° phase difference between the pulse cross correlation and the beating, which is a direct manifestation of the 90° phase difference between the real and the virtual amplitudes.

In Fig. 1(b), we schematically describe our experimental setup. Thirty femtosecond pulses from a

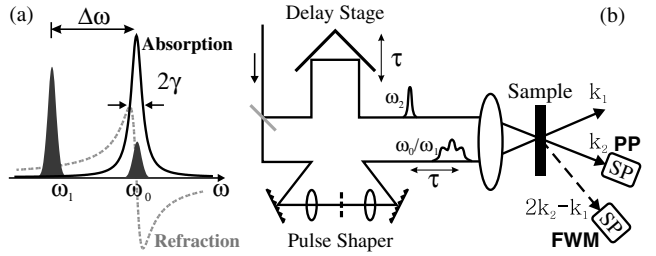

FIG. 1. (a) Schematic diagram of the experiments for a simple two-level system whose natural frequency and damping constant are ω_0 and γ, respectively. Real amplitude at ω_0 and a virtual one at ω_1 are simultaneously excited by two-color picosecond pulse. (b) Schematics of the experimental setup describing picosecond/femtosecond PP and FWM. Spectrally broad 30 fs pulses are used as a probe. SP stands for spectrometer.

Kerr-lens-modelocked Ti:sapphire laser are pulse-shaped using a variable double slit, to create a two-color ps pulse. The spectral width of each component for the picosecond pulse was about 1 meV while their peak power is less than 1 MW/cm^2. The corresponding resonant Rabi energy is approximated to be 0.6 meV, which is clearly much smaller than the detuning used in our experiments ranging from 4 to 40 meV. This strongly suggests that indeed we are in the high detuning and low intensity limit. This two-color pump pulse is used to excite both the virtual and real amplitudes simultaneously. Part of the femtosecond beam is used as a probe, in both PP and FWM experiments. A spectrometer is used to detect the signal at the HH exciton resonance for both experiments. The sample used was a high quality GaAs multiple quantum well with well width of 15 nm and with 30 periods. All experiments were performed at 10 K. Femtosecond one-color four-wave mixing shows a single exponential decay with dephasing time of around 1 ps, which suggests that we are in the Markovian regime.

Shown in Fig. 2(a) are time-integrated FWM experimental data for different relative field strengths I_1/I_0, where I_1 and I_0 are the intensity of ω_1 and ω_0 frequency components, respectively. For comparison, the cross correlation between combined ω_0/ω_1 pulse and the short ω_2 pulse is also shown. When the ω_0 and ω_1 components have comparable strengths, the FWM signal shows little oscillation, whereas the pulse shape in the cross correlation shows pronounced oscillation. As we increase the virtual component ω_1, the oscillation becomes much more visible for the FWM signal, while the pulse shape becomes less oscillatory. Note that at the largest ratio used, $I_1/I_0 = 200$, the beating becomes smaller again. The oscillation period exactly matches the detuning between the real and imaginary parts of the excitation pulse.

However, the most intriguing aspect of the data is the 90° phase shift between the oscillations in the TI-FWM signal and cross correlation. The use of a spectrometer to spectrally select the signal from only the HH exciton shows that the oscillations are not just due to

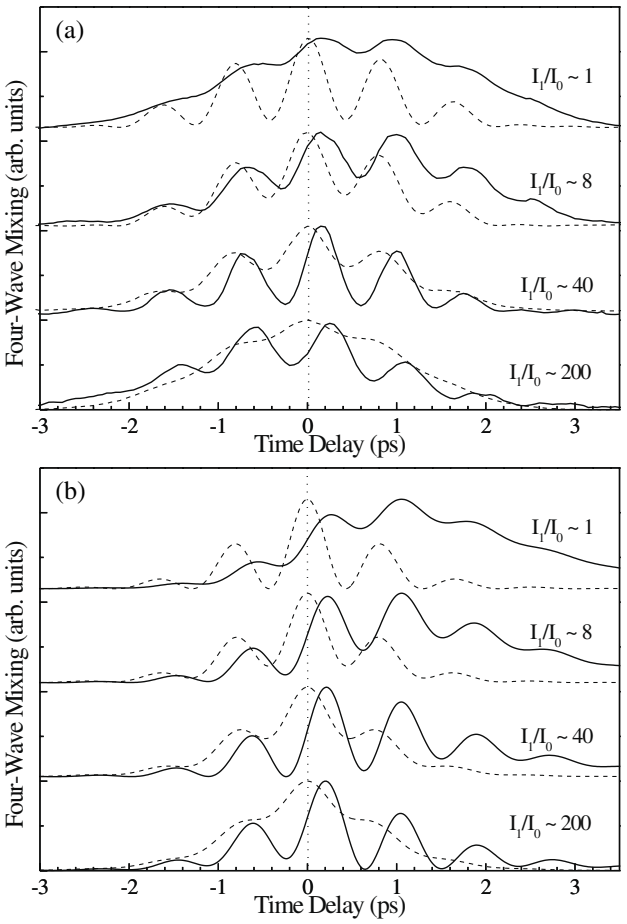

FIG. 2. (a) TI-FWM (solid lines) versus delay for four different relative strengths of I_1/I_0. The pronounced beatings are observed, whose periods of oscillations (0.85 ps) correspond to the inverse of the detuning (4.8 meV). The depth of oscillation increases to a certain point (top three), after which it gets weaker again (bottom). Cross-correlation traces are shown for comparison (dashed lines) (b) Numerical calculation of TI-FWM for a two-level system with pulse parameters that match the experiment.

electromagnetic interference between the resonant and off-resonant polarizations induced by the ω_0 and ω_1 components, respectively. This suggests that the excited-state population is actually oscillating due to interference between excitations of virtual and real exciton states, however the phase shift must be explained.

The phase difference as well as the ω_1 intensity dependent oscillatory behavior can be understood in terms of our picture of the simultaneously excited virtual and real amplitudes interfering with each other. Starting from Eq. (1), neglecting phase relaxation and considering only the oscillatory part and not the envelope function, the excited-state population in our experiments can be approximated by

$$|\Psi_{\text{real}} + \Psi_{\text{virtual}}|^2 \propto \left| \sqrt{I_0}\frac{e^{i\omega_0 t}}{i\gamma} + \sqrt[1]{I_1}\frac{e^{i\omega_1 t}}{\Delta\omega} \right|^2, \quad (2)$$

while the pulse is present and at large enough detuning for ω_1, and where Ψ_{real} and Ψ_{virtual} are wave functions of real and virtual amplitudes, respectively. The modulation we see in FWM is then explained simply by the "steady state" interference of the real and virtual amplitudes. Since the steady-state pulse shape is given by

$$|E_0 + E_1|^2 \propto |\sqrt{I_0}e^{i\omega_0 t} + \sqrt{I_1}e^{i\omega_1 t}|^2, \quad (3)$$

the phase difference of 90° can be explained simply by the fact that there exists a 90° phase difference between the real and the virtual amplitudes.

This simple discussion can also explain the ω_1-intensity dependence. Initially at comparable ω_1 and ω_0 intensities, Ψ_{virtual} is much smaller than Ψ_{real}, and therefore the modulation of FWM signal is small. As the virtual component increases in intensity, Ψ_{virtual} becomes comparable to Ψ_{real} and we observe pronounced beating. Eventually, Ψ_{virtual} becomes stronger than Ψ_{real} and then the oscillation begins to be less dramatic. Because the virtual amplitude survives only during the presence of the ω_1 component, at $t > 2$ ps, the oscillation disappears.

To provide a more detailed comparison than this simple model, we show theoretical calculations of the TI-FWM signal in Fig. 2(b). These calculations are a numerical solution to the optical Bloch equations for a two level system. Since the finite spectral width and detuning of the incident pulses are crucial, we perform calculations based on a spatial Fourier expansion of the optical field and the components of the density matrix. This yields a set of coupled differential equations that are solved using standard numerical techniques. The spectral selectivity of the detection is included in the results by computing the spectrum at each delay and integrating over a 4 meV slice centered at the resonance frequency.

Examination of the excited-state population in the calculation shows that it does oscillate (not shown), in agreement with the simple model. Differential transmission (pump-probe) measurements provide experimental confirmation that the excited-state population is actually oscillating (Fig. 3). The signal is modulated more as the virtual component becomes stronger, until a point is reached, after which the modulation becomes weaker again. Just as in the FWM signal, there also exists a definite phase difference between the cross correlation and the oscillation of the PP signal. It is clear that in all cases the phase shift is approximately 90°.

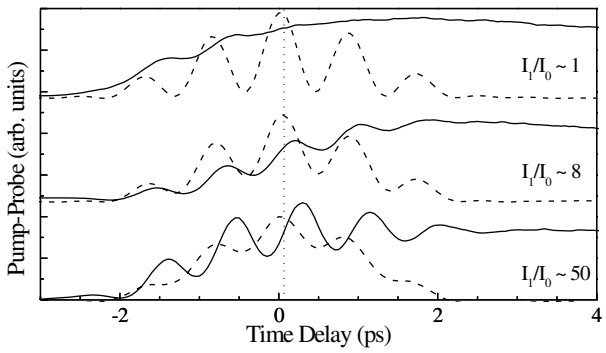

FIG. 3. Differential transmission for three different I_1/I_0.

Verification that inteference between amplitudes is occurring can be obtained by making both amplitudes virtual. We can make both amplitudes predominantly virtual simply by detuning ω_0 away from the resonance, as shown in the inset of Fig. 4(a). As the detuning increases up to one full-width-half-maximum (FWHM) of the HH exciton, the phase difference is much closer to zero than to 90°, as shown in Fig. 4(a). Our numerical results shown in Fig. 4(b) closely match the experiments.

As mentioned above, these phase shifts must be taken into account in coherent control experiments [2–6]. Indeed, this has recently been observed in coherent control experiments that used shaped ultrafast pulses to control population transfer in Li_2 [25]. These experiments indirectly show the virtual-real phase shift by finding that a 90° phase shift between resonant and off-resonant components of the pulse are required to optimize the population transfer. In such complex systems as molecules, however, the optimization of coherent control has been achieved using the various types of learning

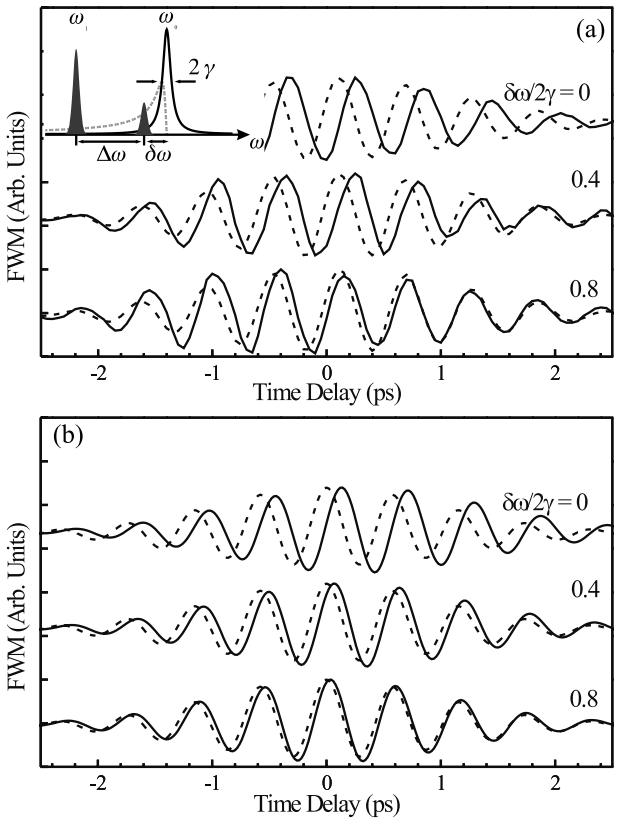

FIG. 4. (a) The oscillatory parts in FWM are shown for the three different $\delta\omega$'s. $\Delta\omega$ is fixed at 7.1 meV and the magnitude of γ is estimated to be 1 meV. The overall phase changes are observed from 90°(up) to 0°(bottom) for the increasing value of $\delta\omega$. (b) Numerical calculation for the same conditions.

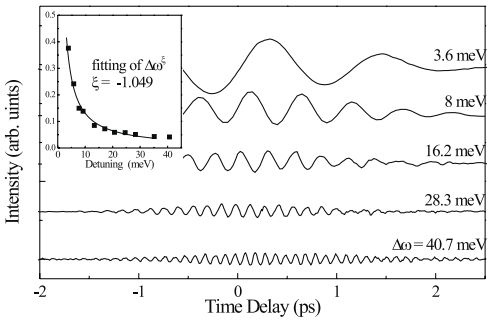

FIG. 5. The oscillatory parts in the FWM signal are shown for various detunings from 3.6 meV (top) to 40.7 meV (bottom). The frequency of the beating follows exactly $\Delta\omega$, while their depth of oscillation decreases with $\Delta\omega$. (inset) The plot for the magnitude of virtual amplitude versus $\Delta\omega$, normalized to the resonant real amplitude.

algorithm. These techniques have been further extended to control the nonlinearities of the continuum and the two photon absorption in semiconductors [26,27]. Our technique, however, could be applied to optimize the coherent control in a predictable way for any optically driven resonance. We now discuss the detuning dependence of our oscillation.

Figure 5 shows the oscillatory parts in the FWM data as a function of the detuning $\Delta\omega$, fixing ω_0 and ω_1 intensities constant. The oscillation amplitude decreases with increasing detuning. This is because the virtual amplitude decreases with the increasing detuning. Therefore, the data shown in Fig. 5 reflect precisely how the virtual amplitude behaves as a function of detuning. Our experiments provide a new and direct way of measuring the virtual amplitude normalized to the real amplitudes. In the inset to Fig. 5, we plot the strength of the virtual amplitude deduced from the depth of the oscillation signal as a function of detuning. The strength decreases approximately as $1/\Delta\omega$, as we would expect from a simple two level system. Therefore, we can say that excitons at our range of detuning behave more or less as a two level atom as far as the virtual amplitude is concerned, and that the contribution from the free carrier continuum to the virtual amplitude might be negligible.

In conclusion, we have demonstrated that it is possible to observe quantum interference between real and virtual amplitudes. These are created by resonant and off-resonant excitation, respectively, of the exciton resonance in a GaAs quantum well. We demonstrate that it is possible to directly probe the magnitude of the virtual amplitude through the corresponding oscillations in the transient four-wave mixing signal or pump-probe signal. This gives a unique tool for examining the interplay between real and virtual amplitudes and enables us to visualize the excited-state quantum amplitudes under off-resonant excitation, as well as their phases. The data closely match calculations using the Optical Bloch equations for a two level system. This indicates that this technique is general and it should be applicable to any resonant system, not just semiconductors.

The work in Korea was supported by MOST (NRL program) and KOSEF (SRC program) and that in Colorado from NIST and NSF.

*Electronic address: denny@phya.snu.ac.kr

[1] M. Sargent, M. O. Scully, and W. E. Lamb, *Laser Physics* (Addison-Wesley, Reading, MA, 1974).
[2] D. Meshulach and Y. Silberberg, Nature (London) **396**, 239 (1998).
[3] N. Dudovich *et al.*, Phys. Rev. Lett. **86**, 47 (1999).
[4] T. Brixner *et al.*, Nature (London) **414**, 57 (2001).
[5] H. U. Stauffer *et al.*, J. Chem. Phys. **116**, 946 (2002).
[6] D. Oron *et al.*, Phys. Rev. Lett. **88**, 063004 (2002).
[7] R. G. Brewer and R. L. Shoemaker, Phys. Rev. Lett. **27**, 631 (1971).
[8] P. M. Farrel, W. R. Macgillivray, and M. C. Standage, Phys. Lett. **107A**, 263 (1985).
[9] Y. S. Bai, A. G. Yodh, and T. W. Mossberg, Phys. Rev. Lett. **55**, 1277 (1985).
[10] J. Y. Bigot *et al.*, Phys. Rev. Lett. **70**, 3307 (1993).
[11] S. Zamith *et al.*, Phys. Rev. Lett. **87**, 033001 (2001).
[12] D. Fröhlich, A. Nöthe, and K. Reimann, Phys. Rev. Lett. **55**, 1335 (1985).
[13] A. Mysyrowicz *et al.*, Phys. Rev. Lett. **56**, 2748 (1986).
[14] S. Schmitt-Rink and D. S. Chemla, Phys. Rev. Lett. **57**, 2752 (1986).
[15] M. Combescot and R. Combescot, Phys. Rev. Lett. **61**, 117 (1988).
[16] R. Zimmermann and M. Hartmann, Phys. Status Solidi (b) **150**, 365 (1988).
[17] W. H. Knox *et al.*, Phys. Rev. Lett. **62**, 1189 (1889).
[18] C. Ell, J. F. Müller, K. El Sayed, and H. Haug, Phys. Rev. Lett. **62**, 304 (1989).
[19] R. Binder *et al.*, Phys. Rev. Lett. **65**, 899 (1990).
[20] S. T. Cundiff *et al.*, Phys. Rev. Lett. **73**, 1178 (1994).
[21] D. S. Kim *et al.*, Phys. Rev. Lett. **80**, 4803 (1998).
[22] Y. H. Ahn *et al.*, Phys. Rev. Lett. **82**, 3879 (1999).
[23] H. Haug and S. W. Koch, *Quantum Theory of the Optical and Electronic Properties of Semiconductors* (World Scientific, Singapore, 1994), 3rd ed.
[24] D. S. Chemla and J. Shah, Nature (London) **411**, 549 (2001).
[25] J. B. Ballard, H. U. Stauffer, E. Mirowski, and S. R. Leone (to be published).
[26] J. Kunde *et al.*, Appl. Phys. Lett. **77**, 924 (2000).
[27] U. Siegner *et al.*, Opt. Lett. **27**, 315 (2002).